Measuring transport anisotropy in Cu/Si multilayers using weak localization

1996 J. Phys.: Condens. Matter 8 1389

(http://iopscience.iop.org/0953-8984/8/10/011)

J. Phys.: Condens. Matter **8** (1996) 1389–1401. Printed in the UK

Measuring transport anisotropy in Cu/Si multilayers using weak localization

A N Fadnis and David V Baxter
Department of Physics, Indiana University, Bloomington, IN 47405, USA

Received 14 August 1995, in final form 5 December 1995

Abstract. We have determined the anisotropy of electron transport in a series of Cu/Si multilayers, by measuring their low-temperature transverse magnetoresistance due to weak localization (WL). For each sample, the measurements were carried out for two different orientations of the applied magnetic field: parallel and perpendicular to the plane of the sample film. Using an analysis based on an anisotropic 3D theory of WL we find that the ratio of the in-plane and out-of-plane components of the electron diffusivity, $\delta = (D_{xx}/D_{zz})$, varies from essentially 1 to more than 2 as the ratio of the Cu to Si nominal layer thicknesses is increased. X-ray diffraction studies indicate the formation of a copper silicide at the interfaces of the multilayers, and a simple stratified conductor model based on this provides an estimate of the anisotropy that is consistent with that measured through the magnetoresistance. In some samples the magnetoresistance shows departures from the expected WL behaviour that are consistent with the presence of superconducting fluctuations.

1. Introduction

Metallic multilayers provide a convenient laboratory for studying many of the generic properties of nanostructured materials since their structure may be easily varied in a controlled manner during deposition. The structure of multilayers is far more easily quantified than that of more general nanostructured materials as well, since their periodic structure makes diffraction experiments quite powerful. In studies of transport in materials with such a large concentration of interfaces the role played by those interfaces is particularly important, but generally quite difficult to study. The importance of interfacial scattering has been clearly identified in the case of the giant magnetoresistance (or GMR) effect discovered recently in nanophase magnetic materials [1] but scattering at the interfaces clearly should dominate the transport properties of other nanostructured materials as well. One experimental probe which holds some promise of being able to shed light onto the role of interfacial scattering in non-magnetic systems is the measurement of transport anisotropy in multilayers.

In earlier work on Cu/Al multilayers [2] we have demonstrated that the study of weak-localization (WL) effects in metallic multilayers can be used to measure the anisotropy of electron diffusivity within the layered structure. A detailed description of the method may be found in [2]. For the purposes of the present discussion we point out that the anisotropy shows up as different characteristic field scales in the WL magnetoresistance for two different orientations of the applied field with respect to the sample plane (either parallel or perpendicular). Weak localization refers to a change in conductance due to a quantum interference between alternate electron diffusion paths in a disordered material.

0953-8984/96/101389+13$19.50

The characteristic fields mentioned above correspond to diffusion lengths associated with the dephasing of this interference by the applied field. Since we use the applied field to provide directional information, we are able to probe transport in the growth direction even though the overall measuring current remains in the plane of the film.

In the present work, we report on the application of this technique to a series of sputtered Cu/Si multilayers. In this system we are able to obtain an independent estimate of the anisotropy using a crude stratified conduction model for the modulation wavelength dependence of the transport, and the predictions of this model are consistent with the anisotropy determined from the magnetoresistance. Other authors [3] have measured magnetoresistance due to WL in noble-metal/Si multilayers previously, and have shown that the results of such measurements can be used to study qualitatively the 2D-to-3D crossover in these systems. However, this earlier work did not obtain a quantitative measure of anisotropy in their 3D samples, and it is just such a quantitative study that is the purpose of the present work. In our case, the going over from Cu/Al to the Cu/Si system was motivated by some additional considerations. Replacing Al by Si is expected to give samples with greater disorder and thereby increase the size of both the magnetoresistance and the characteristic field scales. At the same time, this increase in disorder should also eliminate the need to include a conventional $(\omega_c\tau)^2$ correction term to the magnetoresistance, as was required to describe the measurements in the Cu/Al system. All of these should make the measurement more reliable in the present system than was seen in the Cu/Al study. It was also hoped that the substitution of Si for Al would eliminate the complications associated with superconducting fluctuations (present in the earlier work) which introduce a competing contribution to the magnetoresistance and therefore interfere with the analysis. Unfortunately, the Cu/Si system also exhibits the characteristic behaviour of superconducting fluctuations (presumably due to the formation of a superconducting Cu–Si alloy) and therefore, as is discussed at greater length below, this system is not well suited to a quantitative study of the effects of dimensionality crossover.

A detailed discussion of the phenomenon of WL, as well as the theoretical formalism for calculating the magnetoresistance due to WL, can be found in some excellent review articles [4, 5]. The standard 3D theory of WL needs to be modified in order to be applicable to an anisotropic system such as a multilayer. In our earlier paper [2] we showed that incorporating the anisotropy in the formalism, following the approach of Bhatt *et al* [6], leads to a magnetoresistance that depends on the orientation of the magnetic field, and has the following form:

$$\left(\frac{\Delta\rho}{\rho}\right)_{WL} = \alpha \; \frac{e^2}{2\pi^2\hbar}\sqrt{\frac{eB}{\hbar}}\;\left[\frac{1}{2}\; f_3\left(\frac{B}{B_\phi}\right) - \frac{3}{2}\; f_3\left(\frac{B}{B_\phi + 4/3B_{so}}\right)\right] \qquad (1)$$

where f_3 is the Kawabata function [2, 7, 8]. In equation (1), B is the applied field, α involves the product of the sample resistivity and the ratio of components of the electron diffusivity, and B_ϕ and B_{so} are the characteristic phase coherence and spin–orbit scattering fields respectively. The characteristic fields are defined by the relations $B_\phi = \hbar/4eD\tau_\phi$ and $B_{so} = \hbar/4eD\tau_{so}$, where D is the effective electron diffusivity in a plane perpendicular to the applied field, and τ_ϕ and τ_{so} are the dephasing and spin–orbit scattering times respectively. The orientation dependence of the magnetoresistance comes from the different effective diffusivities entering into the the quantities α, B_ϕ and B_{so} for different orientations of the field. For the two orientations of the field used in our measurements, namely, parallel and perpendicular to the sample plane, these quantities are related to the components of the diffusivity in the following way (note that the power on the ratio involving the prefactor,

α, was given incorrectly in [2]):

$$\frac{D_{xx}\ (= D_{yy})}{D_{zz}} = \left(\frac{[B_{so}]_{\parallel}}{[B_{so}]_{\perp}}\right)^2 = \left(\frac{[B_{\phi}]_{\parallel}}{[B_{\phi}]_{\perp}}\right)^2 = \left(\frac{[\alpha]_{\perp}}{[\alpha]_{\parallel}}\right)^4. \tag{2}$$

Here, the subscripts $\parallel$ and $\perp$ refer to the orientation of the magnetic field with respect to the sample plane, and $\hat{z}$ is the growth direction of the film. In fitting equation (1) to the magnetoresistance data for the two orientations, parameters α, B_{ϕ} and B_{so} are treated as adjustable parameters and the anisotropy is obtained from them using equations (2).

The expression for magnetoresistance given by equation (1) is similar to the one obtained by Szott *et al* [9] for semiconductor superlattices when the appropriate limits are considered. The main difference, however, is that Szott *et al* obtained an expression for the electron diffusivity, and hence the prefactor α, in terms of the physical characteristics of the superlattice such as the miniband width. We treat the quantities α as well as B_{ϕ} and B_{so} as phenomenological parameters to be obtained from the fits and related to the components of the electron diffusivity tensor. For metallic multilayers with relatively small anisotropy it is reasonable to expect the prefactor to be related to the diffusion anisotropy rather than the miniband structure which is unlikely to be well developed in these materials.

2. Experiment

All samples were prepared by planar magnetron rf sputter deposition onto sapphire substrates at ambient temperature. The base pressure of the deposition chamber was 5×10^{-8} Torr with the cryopump throttled and a liquid nitrogen trap filled, and the sputtering pressure was 6.4×10^{-3} Torr of Ar (5N5 purity). The deposition rates were controlled by feeding constant RF power into the sources and the deposition was monitored with quartz oscillators. The targets were purchased commercially (CERAC Manufacturers) and had a specified purity of: Cu: 99.999%; Si: 99.999%. The use of high-purity materials is essential for these studies because a very small concentration of magnetic impurities can significantly distort the measured magnetoresistance in three dimensions [8].

The structure of the samples was characterized with a Scintag-XDS 2000 x-ray diffractometer using Cu Kα radiation at both small and large angles. The modulated structure was created by using a rotating carousel to expose the substrates to each source in turn with the exposure time being determined by the speed of rotation. By using two or three different speeds in each rotation, thereby making several different samples in each run, we are able to estimate the individual layer thicknesses for each sample from the measured modulation wavelengths. Figures 1(a) and 1(b) show the low- and high-angle x-ray diffraction data respectively. The low-angle superlattice peaks clearly visible in figure 1(a) indicate that there is a well defined electron-density modulation in all the samples. The modulation wavelength was determined by fitting these low-angle peak positions to Bragg's law as modified to account for refraction [10], and the total thickness is taken as the number of periods times this value. In all cases the modulation wavelength was within 5% of its nominal value. The high-angle data are characterized by a broad maximum near the position of the copper(111) peak. In most samples this peak consists of an unresolved doublet, presumably indicating that metallic Cu and a Cu silicide are both present in the sample. Other authors have recently explored Cu silicide formation in the context of the application of Cu metallization in Si integrated circuits. It has been reported that the η' or η'' structure of Cu_3Si is the phase that forms from the solid-state reaction of Cu and Si [11]. The diffraction patterns that we see are consistent with this description; however, the peaks

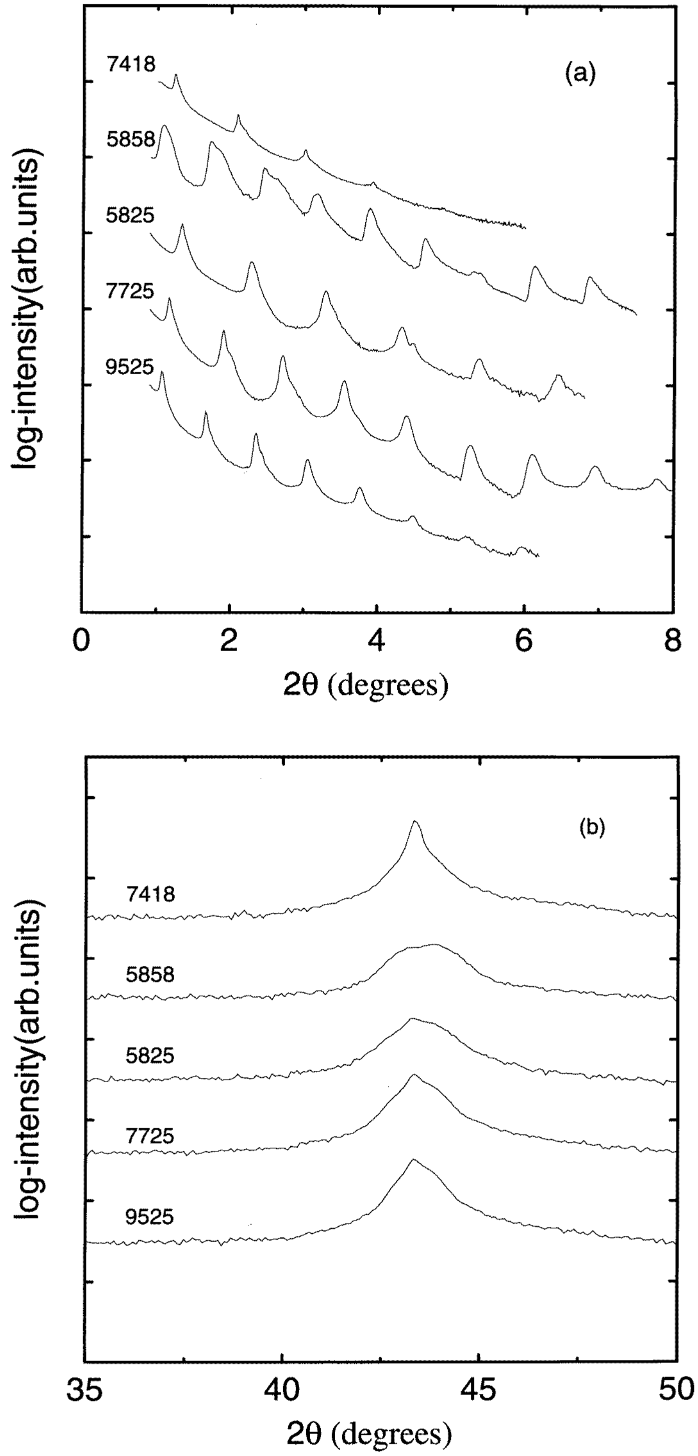

Figure 1. (a) and (b) are the x-ray diffraction patterns of the samples studied at low and high angles respectively using Cu Kα radiation. The presence of sharp peaks in the low-angle data indicates the structural anisotropy in the multilayers. In (b), all samples except number 7418 show evidence of two broad peaks, suggesting silicide formation at the interfaces.

from our samples are too few and too broad to allow for unambiguous identification of the silicide phase.

The sample magnetoresistance was measured with a high-precision, four-terminal, ac bridge in a ^{4}He Dewar equipped with a superconducting magnet as described in our previous publications [2, 12]. Measurements were made for temperatures from 2.5 K to 20 K, and in fields ranging from 0 T to about 8 T. In each case, a negative-field sweep was carried out for at least one temperature to ensure that there was no Hall contribution to the measured resistance due to possible sample inhomogeneities.

Table 1. Physical parameters for the samples studied. Uncertainties are ρ: ±5%; Λ: ±3 Å $t_{\mathrm{Cu,Si}}$: ±5 Å. Other parameters include the ratios of the intensities (I_1/I_2) of the two peaks visible in the high-angle x-ray data. The thicknesses of the high-conductivity (metallic) and the low-conductivity (silicide) layers, s_{m} and s_{s} respectively, are calculated from the ratio I_1/I_2 and the measured value of Λ, and the last column gives the resistivity of the metallic layer in each sample estimated using the model described in the text with the silicide layer assumed to have a resistivity of 190 $\mu\Omega$ cm.

Sample	d (Å)	Λ (Å)	$t_{\mathrm{Cu}}/t_{\mathrm{Si}}$ (Å/Å)	L/w	$\rho_{\parallel}$(4.2 K) ($\mu\Omega$ cm)	I_1/I_2	s_{m} (Å)	s_{s} (Å)	ρ_{m} ($\mu\Omega$ cm)
9525	4200	120	95/25	2.5	30.5	3.2	91	29	24±1
7725	3570	102	77/25	2.5	46.2	2.6	74	28	36±2
5825	2905	83	58/25	2.7	79.4	2.0	55	28	61±4
5858	4060	116	58/58	2.6	159	0.6	43	73	124±15
7418	4140	92	74/18	11.6	51.3	*	72*	20*	43±4

* The high-angle x-ray data corresponding to sample 7418 did not show two peaks. For this sample, we approximate s_{s} by assuming that the ratio $s_{\mathrm{s}}/t_{\mathrm{Si}}$ is the same as seen for the samples with 25 Å Si layers and compute ρ_{m} on this basis.

The physical characteristics of the samples studied are summarized in table 1. The samples are identified by the nominal thicknesses of their elemental layers (thus sample 9525 was made with bilayers consisting of 95 Å of Cu and 25 Å of Si). All samples were made with 35 bilayers with the exception of sample 7418 which has 45 bilayers. The first seven columns of table 1 list experimentally determined quantities describing the structure of the samples, with I_1/I_2 being the intensity ratio of the two subpeaks seen in the high-angle x-ray diffraction pattern as discussed above. This ratio was determined by fitting the unresolved peaks to a pair of split Pearson line shapes using the standard Scintag software. The remaining columns of the table relate to a model of the sample resistivity that is discussed below.

3. Results and discussion

Figure 2 shows the temperature dependence of the Cu/Si multilayers studied for temperatures between 1.5 K and 40 K. It is quite similar to that typically observed in the case of amorphous metallic alloys and is also similar to the temperature dependence of resistivity observed in Cu/Al multilayers studied previously. Here we do not intend to extract any quantitative information from the temperature dependence, but use it merely to point out qualitatively the disordered character of our multilayers. The trend of this low-temperature behaviour with overall sample resistivity is consistent with that seen in typical disordered metals, indicating the importance of quantum corrections to the low-temperature conductivity of these samples.

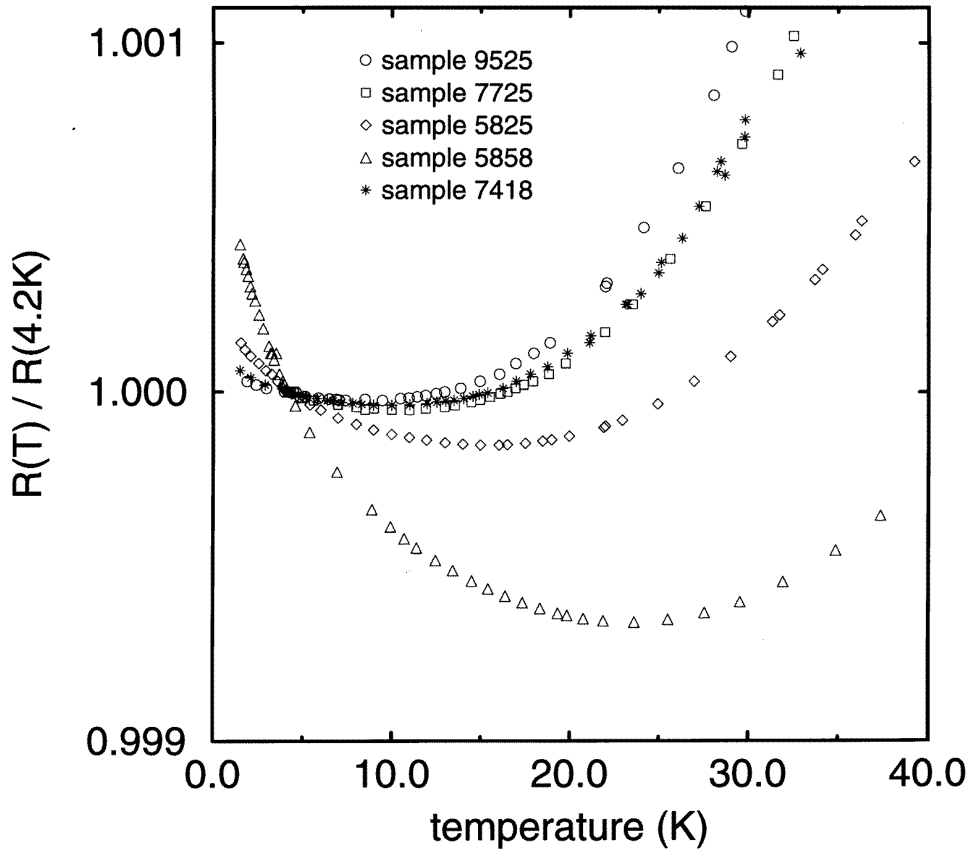

Figure 2. The resistance of each of the Cu/Si multilayers studied, normalized with respect to its value at 4.2 K, is plotted as a function of temperature. The effects of the quantum corrections to the conductivity, similar to those seen in disordered metals, are clearly visible in the data below 20 K.

Magnetoresistance data for all of the samples studied are displayed in figures 3(a)–3(e). The circles show the data for the case with the magnetic field in the plane of the sample film, the crosses that with the field perpendicular to the film, and the solid lines show the fits obtained using equation (1). The details of the fitting procedure are described in our earlier publications [2, 12] and are summarized below. The experimental data are seen to agree quite well with the fits, except for the low-temperature data (6.5 K and below) for some samples.

Comparing these data with the Cu/Al multilayer data we reported earlier [2], we notice that the magnetoresistance behaviour in the two cases is qualitatively very similar, and conforms to the predictions of WL. As expected, however, the total change in resistance for a given range of field is greater, and the anisotropy is more clearly evident in data for the Cu/Si multilayers than the case for our earlier study of Cu/Al multilayers. Furthermore, the fits to WL theory agree with the data at high fields to a much greater degree in the present case than was seen for the Cu/Al multilayers. This indicates that the conventional $(\omega_c\tau)^2$ correction which was necessary to achieve satisfactory agreement between theory and data at

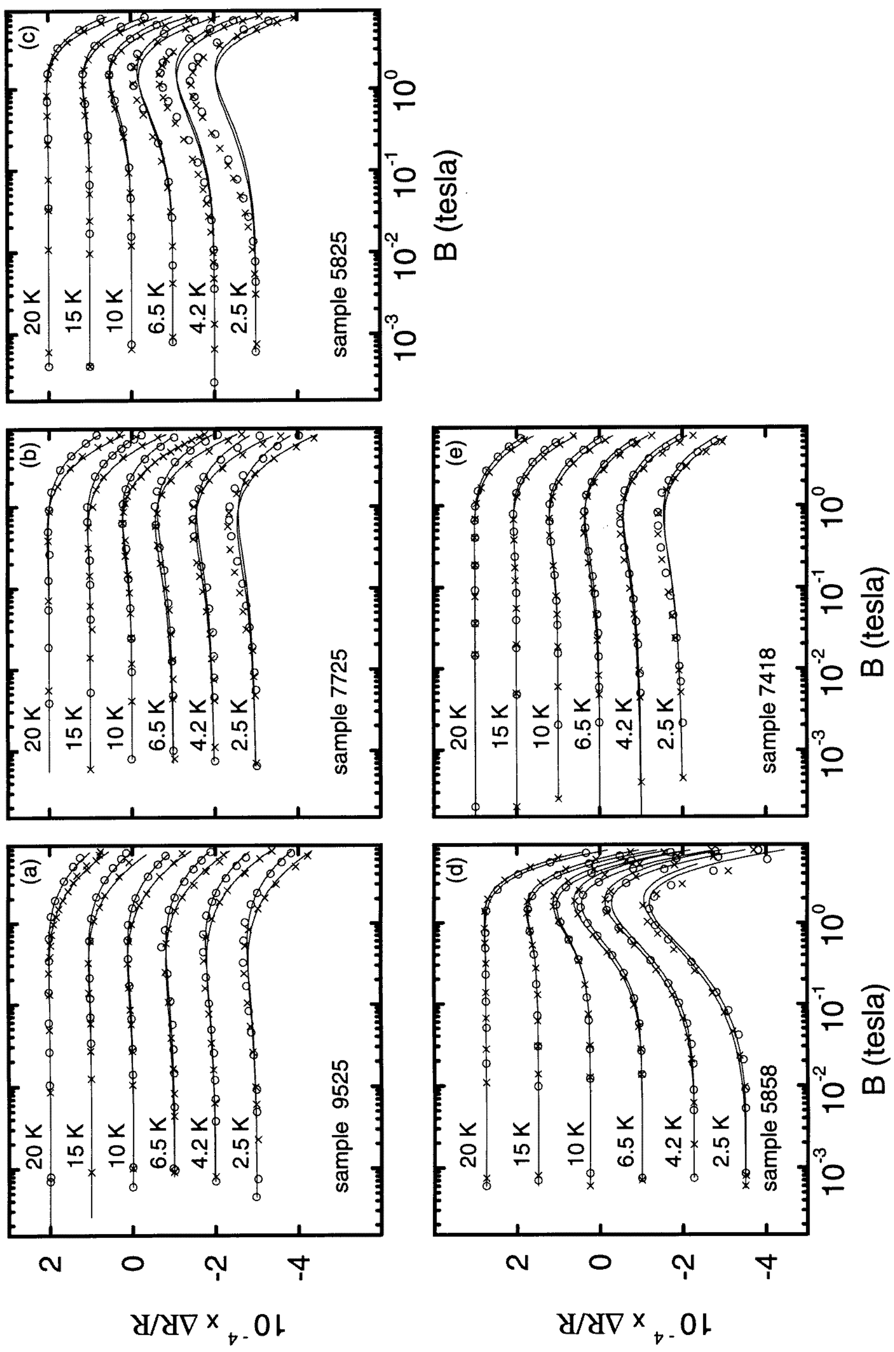

Figure 3. The magnetoresistance data for all the Cu/Si multilayers studied, for temperatures from 2.5 K to 20 K, are shown in (a)–(e). For each temperature, the magnetoresistance is normalized with respect to the zero-field resistance at that temperature. The data are decimated and offset along the y-axis for clarity. The circles show the data with the field in the plane of the film, the crosses that with the field perpendicular to the film, and the lines show the fits obtained using equation (1).

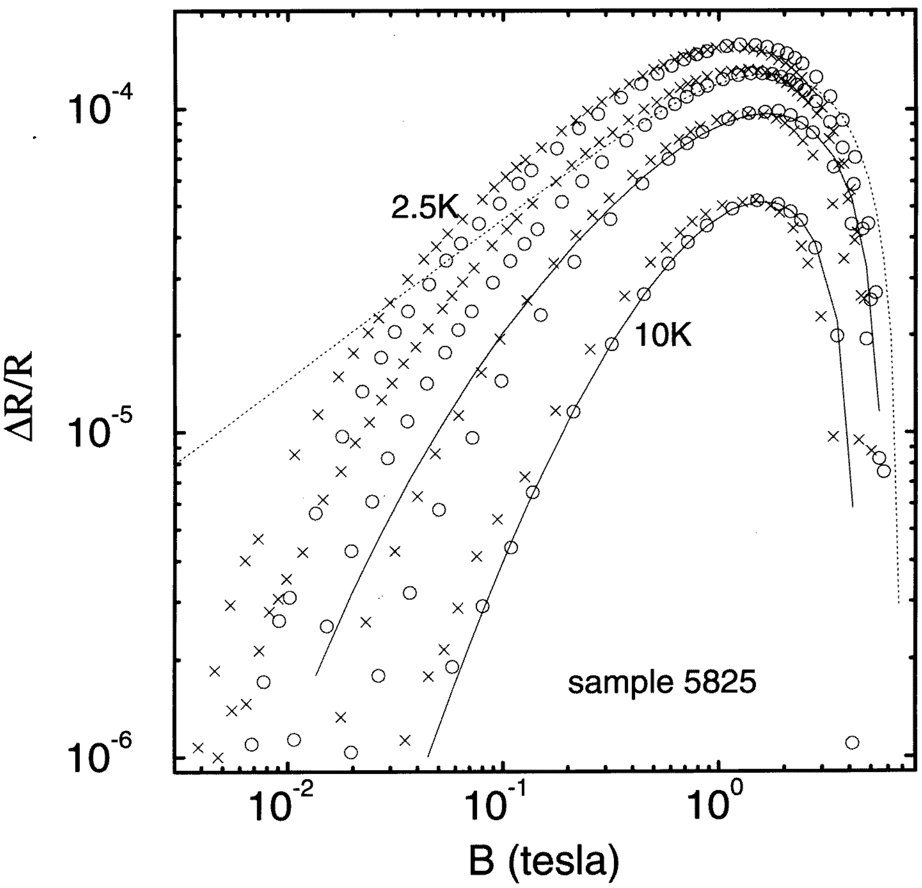

Figure 4. The low-temperature (2.5 K, 4.2 K, 6.5 K and 10 K) magnetoresistance data for a representative sample (5825) shown on a log–log plot. Once again the circles represent the data with the field in the plane of the film, the crosses that with the field perpendicular to the film, and the lines show the fits for the case of the field in the plane of the film. The theory curve shown by the dotted line is obtained by setting B_ϕ to zero (its ideal zero-temperature limit). The inadequacy of the theory as regards describing the low-temperature data is clearly revealed. As discussed in the text, the primary source of this failure is the presence of superconducting fluctuations in these samples.

high fields in the case of the Cu/Al system is not required here. The disagreement between the experiment and theory at low temperatures (most obvious for samples 7725 and 5825) is also similar to that seen in Cu/Al multilayer data. This discrepancy is shown in greater detail for sample 5825 in figure 4. For clarity, in this figure, only theory curves corresponding to the data with the field in the plane of the sample film are shown. The dotted line is the theory curve obtained by setting the B_{so}- and α-values to those obtained from the fits to the data above 6.5 K, while setting the B_ϕ-value to zero. Since zero is the smallest physically acceptable value for B_ϕ, the inadequacy of the theory as regards describing the data below $T = 6.5$ K is quite clearly demonstrated. We do note, however, that the qualitative behaviour of the low-temperature data is still very similar to that seen at higher temperatures (in terms of the difference between the data for the two field orientations).

In our study of Cu/Al multilayers, we argued that the presence of superconducting fluctuations (Al being the source of superconductivity) was one of several possible causes of a similar discrepancy seen in that case. Of relevance to the present case is our recent observation of superconducting fluctuations in Ge/Cu/Ge and Si/Cu/Si sandwich structures [13] (indicating T_cs of roughly 400 mK and below 300 mK respectively). The behaviour of sample 5825 is very characteristic of a sample exhibiting superconducting fluctuations. It is thus most likely that superconducting fluctuations are primarily responsible for the low-temperature discrepancy seen in these samples and that 5825 (which shows the greatest discrepancy) has the highest transition temperature among those samples shown in figure 3. It is, however, important to note that the theory that we use to analyse our data must fail in the limit of large anisotropy, since in this limit the field dependence should cross over to the two-dimensional form which involves digamma functions rather than f_3 [4]. More experiments are needed to quantify these effects due to dimensionality crossover but the formation of metallic silicides and the presence of superconducting fluctuations in the Cu/Si system makes it unsuitable for such a study. Ag/Ge multilayers, which exhibit no signs of superconductivity, are more suitable for the quantitative analysis of dimensionality crossover and such a study is currently under way. Preliminary results from this work indicate that crossover effects become significant only for anisotropies of 4 or more, so such effects should not be important in the Cu/Si samples considered here [14].

Table 2. The B_{so}-values obtained by fitting the theory to magnetoresistance data on Cu/Si multilayers for two different orientations of the magnetic field ($\perp$ and $\parallel$ to the field), and the anisotropy ratios ($\delta_{B_{so}}$, δ_α) calculated from them using equation (2). δ_{mdl} is the predicted anisotropy as described in the text.

Sample	$[B_{so}]_\parallel$ (mT)	$[B_{so}]_\perp$ (mT)	$\delta_{B_{so}}$	$\alpha_\parallel$ ($\mu\Omega$ cm)	$\alpha_\perp$ ($\mu\Omega$ cm)	δ_α	δ_{mdl}
9525	157	93	2.8 $\pm$0.8	26.1	32.9	2.5$\pm$1.0	2.10 $\pm$0.2
7725	234	175	1.8 $\pm$0.3	46.6	54.9	1.9$\pm$0.4	1.69 $\pm$0.15
5825	465	388	1.45$\pm$0.1	97.8	101	1.1$\pm$0.2	1.32 $\pm$0.07
5858	490	526	0.9 $\pm$0.1	202	206	1.1$\pm$0.3	1.04 $\pm$0.03
7418	226	188	1.45$\pm$0.1	51.6	49.5	1.2$\pm$0.4	1.46 $\pm$0.15

The fitting procedure used in the analysis of the present data was similar to that described in our study of Cu/Al (see [2]). A preliminary fit to the data at each temperature is made allowing each of the three parameters (α, B_{so} and B_ϕ) to vary. In order to minimize the influence of enhanced inter-electron interactions on the fitting procedure, the fit is not performed over the entire range of magnetic fields for all temperatures. The interaction effects become more important as the ratio B/T increases, and so the fits are made only up to a field set by a specified value of this ratio (typically taken to be 0.4 T K) [12]. In this preliminary fit the values obtained for α and B_{so} typically are constant for the higher-temperature data but change as the temperature falls below 6.5 K. Since these parameters should have no temperature dependence this indicates some contribution from effects other than WL (primarily superconducting fluctuations in these samples). Starting from the values obtained with this preliminary fit, we then obtain the final values for the parameters by optimizing α, B_{so}, and one B_ϕ-value for each temperature, by fitting to several temperatures simultaneously. The influence of the superconducting fluctuations on this fit was minimized by excluding the lower-temperature data (typically those below 6.5 K) from the fit. Since the parameters B_{so} and α are independent of temperature, such

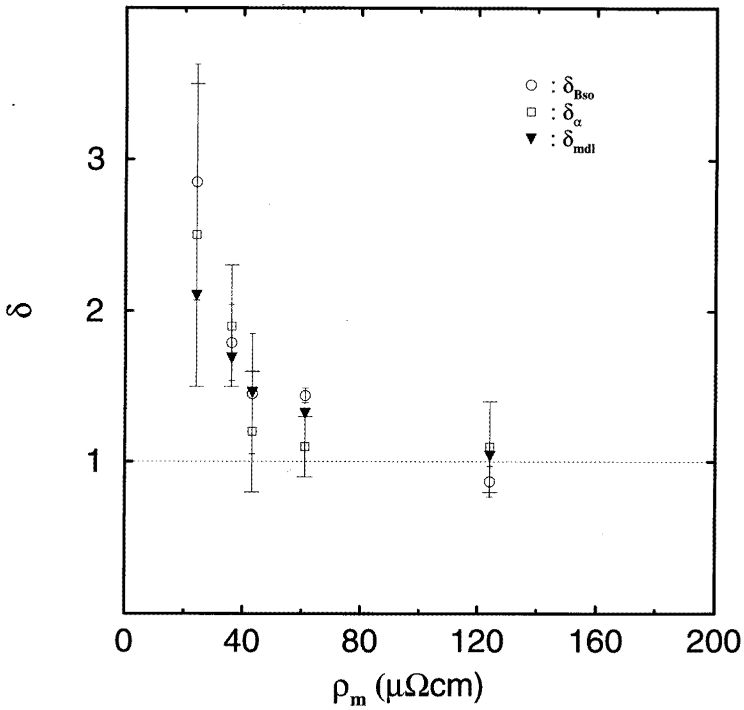

Figure 5. The anisotropy ratios $\delta_{B_{so}} = [B_{so}]^2_{\|}/[B_{so}]^2_{\perp}$ and $\delta_\alpha = [\alpha]^4_{\perp}/[\alpha]^4_{\|}$, obtained from the fits, are plotted against the quantity ρ_{m}, which is the resistivity of the high-conductivity layer in each multilayer, estimated with a stratified conductor model as described in the text. The error bars in the figure indicate the range of values obtained from variations of the fitting procedure, such as changing the range over which the WL fit was performed. The anisotropy predicted from the stratified conductor model (δ_{mdl}, based on measured resistivities and x-ray diffraction data as described in the text) is also plotted. Uncertainties on the model predictions are listed in table 2, but are not shown in the figure in order to avoid undue clutter.

a fit to N different temperatures involves only $N + 2$ free parameters. The B_{so}- and α-values, obtained by fitting equation (1) to the data for the two orientations of the field, are shown in table 2, along with the corresponding anisotropy ratios $\delta_{B_{so}} = ([B_{so}]_{\|}/[B_{so}]_{\perp})^2$ and $\delta_\alpha = (\alpha_\perp/\alpha_\|)^4$. The uncertainties quoted for the parameters obtained from this fitting procedure are determined by observing the range of values obtained under slight variations of the fitting (such as changing the field range over which the WL fit is performed or including additional low-temperature data in the final fit). In all cases the range of values so obtained is larger than the statistical uncertainties obtained from fitting under any one procedure. Thus the uncertainties in our fitting procedure are dominated by the inability of current theory to adequately describe competing contributions to the magnetoresistance. This is most dramatically seen in the case of the values for B_ϕ which typically display large uncertainties in 3D WL measurements [12]. This reflects in part the fact that, unlike values of α and B_{so}, B_ϕ-values are not averaged over several temperatures. In addition to this, however, the statistical uncertainties in the B_ϕ-values are smallest at low temperatures where they are most susceptible to systematic errors due to superconducting fluctuations, errors in determining the zero-field resistance value, and finite-sample-thickness effects [2]. As a result of this, the uncertainties in B_ϕ are too large for an estimation of the anisotropy from this parameter to be possible. The value of α obtained from the fit is also more susceptible to these systematic errors than is that of B_{so} but the overall uncertainty in the ratio $\delta_\alpha = [\alpha]_\perp^4/[\alpha]_\parallel^4$ obtained from the fits is small enough to allow a reasonable prediction for the anisotropy (as shown in figure 5). As we found with Cu/Al, however, the most precise determination for the anisotropy comes from the spin–orbit field and these values too are shown in figure 5. The reason for this can be understood by looking at the data in figure 3. The dephasing field scales with the position at which the data first depart from zero, while the spin–orbit field scales with the position of the positive peak seen at low temperatures. The observation that $\delta_{B_{so}}$ is the most reliable estimate of the anisotropy simply reflects the fact that the position of this positive peak is the feature of the magnetoresistance curve that is least susceptible to the systematic errors discussed above.

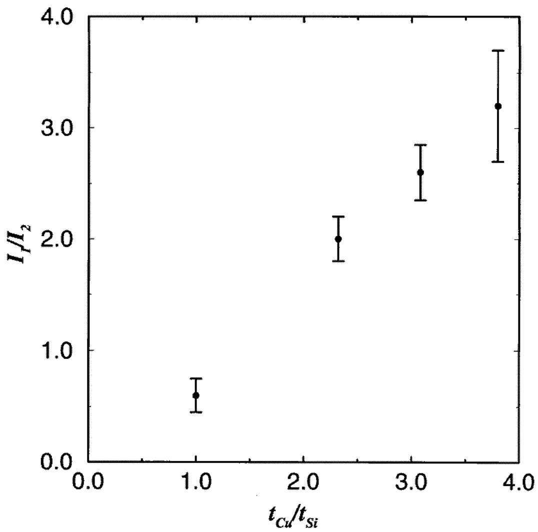

Figure 6. The intensity ratio for the two subpeaks in the high-angle x-ray diffraction pattern (figure 1(b)) versus the ratio of the nominal Cu and Si layer thicknesses for the four samples, showing evidence for the formation of a measurable amount of silicide. The intensity ratio is determined by fitting the peaks shown in figure 2(a) to two peaks and the uncertainties reflect the range of values obtained when fitting with different peak shapes.

In order to understand the dependence of the observed anisotropy on the structure of the multilayers we consider a simple stratified conductor model similar to the one used and discussed by Gurvitch [15]. We assume our multilayers to be made of alternating layers of two different phases: a highly conductive metallic phase (Cu with a small amount of dissolved Si) and a less conductive silicide phase. The true structure of these multilayers is undoubtedly more complicated than this very simple model, but given the large conductivity contrast between Cu- and Si-rich phases this picture should capture the essential physics dominating the transport behaviour in these materials. Using the procedure described earlier for fitting to the high-angle x-ray data we estimate the thickness ratio of the two phases by the intensity ratio of the two components in the main peak. This ratio, combined with the measured modulation wavelength, then allows us to estimate the thicknesses of the two different layers for each sample (denoted s_m and s_s for the metallic and silicide layers respectively in table 1). In principle this intensity ratio is not determined solely by the volume fraction of the two phases; however, figure 6 shows that it does scale well with the nominal Cu and Si thicknesses. Moreover, the silicide thickness derived from this analysis is essentially constant for a constant nominal Si thickness (samples 9525, 7725, and 5825), so we believe the procedure to give a reasonable approximation to the true physical layer thicknesses. By combining this information with an estimate of the silicide layer resistivity (ρ_s) and the measured overall film resistivity ($\rho_\parallel$) we can estimate the resistivity of the metallic layer using the formula [15]:

$$\rho_{\mathrm{m}} = \frac{\rho_{\|}\rho_{\mathrm{s}}s_{\mathrm{m}}}{\rho_{\mathrm{s}}\Lambda - \rho_{\|}s_{\mathrm{s}}}. \tag{3}$$

Thick films of Cu_3Si have been reported to have a resistivity of roughly 60 $\mu\Omega$ cm, and studies have shown this resistivity to be sensitive to exposure to oxygen [16]. A consequence of this large resistivity for Cu silicides is that the resistivity of the silicide layers should be much less sensitive to their thickness than will be the resistivities of the metal layers. Therefore, we further assume that ρ_{s} is the same for all samples in modelling their resistivities.

With these assumptions, equation (3) provides a consistent description of the sample resistivities (i.e. leads to a ρ_{m} that is both positive and less than ρ_{s} for all samples) only if we assume a silicide resistivity greater than 150 $\mu\Omega$ cm. Provided that this limit is respected, the value obtained for ρ_{m} is relatively insensitive to the precise choice made for ρ_{s} or to variations of the x-ray intensity ratio within its range of uncertainty. This limit on the resistivity is certainly greater than the reported 'bulk' resistivity for Cu_3Si but it is not unreasonable for a thin film with a highly disordered structure, and possibly a nonuniform composition, as is expected for these multilayers. Having computed ρ_{m} according to the above prescription, one can then go on to compute the value for the sample resistivity in a hypothetical experiment with the current flowing in the growth direction (the so-called CPP geometry often discussed in GMR studies [17]):

$$\rho_{CPP} = \frac{\rho_{\mathrm{m}}s_{\mathrm{m}} + \rho_{\mathrm{s}}s_{\mathrm{s}}}{\Lambda}. \tag{4}$$

In principle this equation also includes a term from the interface scattering (denoted $AR_{\mathrm{m/s}}$ in [17]) in the numerator. For the present case, the resistance of the layers themselves ($\rho_{\mathrm{s}}s_{\mathrm{s}}$) is roughly an order of magnitude larger than the typical contributions from interfacial resistance, so we ignore the latter in our calculation. The error introduced by this action should be no greater than that introduced by assuming a constant silicide resistivity, and both of these approximations should be negligible compared to the uncertainties in the measured anisotropies. The ratio of this ρ_{CPP} to the normal resistivity ($\rho_{\|}$ in table 1) should be equal to the anisotropy that we have measured using our WL technique if the model described for the conduction is to be consistent. In figure 5 we have plotted the anisotropies derived from the WL measurements (δ_α and $\delta_{B_{so}}$), and that obtained from the above model ($\delta_{\mathrm{mdl}} = \rho_{CPP}/\rho_{\|}$), against ρ_{m}. One can clearly see that as the ρ_{m}-value increases toward the resistivity of the silicide, the anisotropy approaches 1. In particular, when the value of ρ_{m} from the model is 120 $\mu\Omega$ cm or more, the transport becomes isotropic to within our experimental resolution. For lower values of ρ_{m} the measured anisotropy agrees reasonably well with that predicted by the simple stratified conductor model. The predictions for δ_{mdl} plotted in figure 5 are based on the assumption that $\rho_{\mathrm{s}} = 190$ $\mu\Omega$ cm. Changing the assumed value for ρ_{s} by ± 40 $\mu\Omega$ cm does not qualitatively alter the level of agreement between the measured and model values for the anisotropy.

4. Conclusion

We have measured the low-temperature transverse magnetoresistance due to weak localization in a series of sputtered Cu/Si multilayers. As in our earlier work on Cu/Al multilayers, we have shown that such measurements can be used to detect anisotropy in the transport properties of layered materials by exploiting the dependence of magnetoresistance on the orientation of the field with respect to the sample plane. Comparing the present results with those for Cu/Al multilayers, we find that the agreement between the anisotropy predicted from the prefactor (δ_α) and that from the spin–orbit-field scale ($\delta_{B_{so}}$) is better in the present case. We still find that the dephasing field does not provide a reliable determination of the anisotropy however. In this study of Cu/Si, unlike in the earlier work, we were able to obtain an independent estimate of the anisotropy from a simple stratified conduction model and this estimate is consistent with that found from the fits to the magnetoresistance. The experimentally measured values of the anisotropy are seen to vary monotonically with the resistivity of the more conductive of the two materials comprising the multilayer in our simple model, with isotropic behaviour seen as the resistivity of this material approaches that of its less conductive partner in the structure. We believe that the technique used here can be extended to other layered systems as well. It is, however, evident from both the present study and our earlier work on Cu/Al multilayers that further theoretical input is needed regarding the limitations of existing theory in the presence of superconductivity and strong anisotropy.

Acknowledgments

This work was supported by the NSF under contract number DMR93-14018. The authors would like to acknowledge fruitful discussions with John Carini, Gamini Sumanasekara, and Allan H MacDonald.

References

[1] Parkin S S P 1993 *Phys. Rev. Lett.* **71** 1641
[2] Fadnis A N, Trudeau M L, Joly A and Baxter D V 1993 *Phys. Rev.* B **48** 12 202
[3] Audouard A, Kazoun A, Broto J M, Marchal G and Fert A 1990 *Phys. Rev.* B **42** 2728
Cherradi N, Audouard A, Marchal G, Broto J M and Fert A 1989 *Phys. Rev.* B **39** 7424
[4] Bergmann G 1984 *Phys. Rep.* **107** 1
[5] Lee P A and Ramakrishnan T V 1985 *Rev. Mod. Phys.* **57** 287
[6] Bhatt R N, Wölfle P and Ramakrishanan T V 1985 *Phys. Rev.* B **32** 569
[7] Kawabata A 1980 *J. Phys. Soc. Japan* **49** 628
[8] Baxter D V, Richter R, Trudeau M L, Cochrane R W and Strom-Olsen J O 1989 *J. Physique* **50** 1673
[9] Szott W, Jedrezejek C and Kirk W P 1989 *Phys. Rev.* B **40** 1790; 1992 *Superlatt. Microstruct.* **11** 199
[10] Miceli P F, Neumann D A and Zabel H 1986 *Appl. Phys. Lett.* **48** 24
[11] Cros A, Aboelfotoh M O and Tu K N 1990 *J. Appl. Phys.* **67** 3329
[12] Richter R, Baxter D V and Strom-Olsen J O 1988 *Phys. Rev.* B **38** 10 421
[13] Sumanasekara G, Williams B D, Baxter D V and Carini J P 1994 *Phys. Rev.* B **50** 2606; 1993 *Solid State Commun.* **85** 941
[14] Baxter D V, Sumanasekara G and Carini J P 1996 *J. Magn. Magn. Mater.* at press
[15] Gurvitch M 1986 *Phys. Rev.* B **24** 540
[16] Aboelfotoh M O and Krusin-Elbaum L 1991 *J. Appl. Phys.* **70** 3383
[17] Pratt W P Jr, Lee S-F, Holody P, Yang Q, Loloee R, Bass J and Schroeder P A 1993 *J. Magn. Magn. Mater.* **126** 406